

Research Article

On a Novel Topology of Matrix Converter Applied to Accelerator DC Power Supply

Bin Wang ^{1,2}, Weizhang Song ³, and Yang Si ²

¹School of Physics and Electronic-Electrical Engineering, Ningxia University, Yinchuan, Ningxia, China

²New Energy (Photovoltaic) Industry Research Center, Qinghai University, Xining, Qinghai, China

³School of Electrical Engineering, Xi'an University of Technology, Xi'an, Shannxi, China

Correspondence should be addressed to Bin Wang; wangbin053@nxu.edu.cn

Received 24 February 2022; Revised 1 June 2022; Accepted 23 June 2022; Published 13 August 2022

Academic Editor: Jianxiang Xi

Copyright © 2022 Bin Wang et al. This is an open access article distributed under the Creative Commons Attribution License, which permits unrestricted use, distribution, and reproduction in any medium, provided the original work is properly cited.

The current topology schemes of heavy ion accelerator power supply have serious pollution to the power grid caused by low power factor of the grid side. Considering the characteristics of adjustable power factor and bidirectional energy transfer of the matrix converter, the possibility of which applied to the accelerator DC power supply is studied and three kinds of backup topology schemes including the preceding regulated matrix rectifier (MR) are proposed in this article. Given the actual situation of accelerator power supply, research has been focused on the modulation strategy suitable for the topology of the preceding regulated MR and simulation validation. Based on simulation of the preceding regulated MR scheme, a matrix power prototype is developed. A power factor tester is utilized to test grid side power factor. According to the experimental results, it is prospectively feasible to apply the preceding regulated MR topology to accelerator DC power supply, with excellent performance of the grid side.

1. Introduction

At present, heavy ion accelerators are mainly applied in high-energy physics and medical fields. In the heavy ion synchrotron, the heavy ions injected into the accelerator are accelerated in a circular orbit by the strong magnetic field of the magnet. The accelerated high-energy charged particles bombard the nucleus to facilitate the research of the internal structure of the basic particles in the microscopic world. It can be utilized for the treatment of industrial waste and the industrial nondestructive testing by generating of high-energy X-ray. It can also be utilized for treatment of tumors by generating of high-energy ion beams [1–3].

As an important part of the accelerator, the synchrotron field system generates a magnetic field to restrain motion of ion beams in the accelerator. The development of heavy ion accelerators pursues better beam quality and higher beam intensity, which requires lower magnetic ripple and higher magnetic field accuracy of the accelerator magnetic field system. A field system is composed of a magnet and magnetizing power supply. The performances of magnetizing power supply

affect straightforwardly the quality of the magnetic field. Some indicators of the field system, such as ripple and precision of the magnetic field, directly depend on the current ripple and tracking error of magnetizing pulse power supply. Therefore, the accelerator power supply plays an important role in the high-performance support of modern accelerators. With the development of modern accelerator technology, the requirements for beam quality and stability are becoming higher and higher, which means that the performance of magnetizing power supply needs to be improved further accordingly.

The accelerator power supply generally operates in the DC or pulse mode and provides the magnet with a specific magnetizing current to generate the required magnetic field. A hybrid 12-pulse rectification scheme is adopted in some current magnetizing power supplies in heavy ion accelerators [4]. The thyristor phase-controlled rectification and IGBT pulse-width modulation (PWM) transformation technology are used in the synchrotron dipole magnet power supply [5]. The main circuit topology of sextupole magnet digital power supply of Lanzhou heavy ion accelerator (HIRFL-CSR) is prestage uncontrolled rectifier and poststage H-bridge chopper [6].

It can be seen that the accelerator power supply system is usually composed of a three-phase rectifier and a DC/DC converter. The rectifier with an energy storage capacitor in the prestage mostly works in the traditional phase-controlled rectification or uncontrolled rectification mode, which can easily convert the power grid current (AC) into the direct current (DC). However, besides the short lifespan of the DC capacitor of the rectifier, the serious deficiency of the rectifier is that the large amount of harmonic current of the input side inevitably causes the low power factor of the system and the high harmonic distortion rate, bringing great impact to the power grid. In addition, multiple switching converters of series-parallel connection and auxiliary switching phase-shifting drive are usually utilized to improve the equivalent switching frequency. However, it makes the system more complex and high cost [5].

The researches of the superconducting technology and the superconducting materials are another present hotspot in the accelerator field. Superconducting magnets have the advantages of smaller space occupied and higher magnetic field intensity, which can meet the increasingly tough requirements of accelerator magnets. So, they are widely applied by major accelerator research institutions [7–9]. As the superior performance of the superconducting magnet, the magnet and the supporting power supply are becoming a research hotspot in the field of heavy ion accelerators.

In high intensity heavy ion accelerator facility (HIAF) of China, superconducting magnets will be widely applied [10–12]. The superconducting magnet will be connected in series and be powered by a power supply working in the pulse operation mode. When the power supply works in the pulse mode, the output current is a trapezoidal wave, which is divided into five segments: front flat bottom segment, rising segment, flat top segment, falling segment, and rear flat bottom segment, and each segment is smoothly connected by a quadratic curve. The load of pulse superconducting power supply is a series of superconducting magnets, with an inductance of up to several dozens H (Henrys) in typical operation, whereas the load resistance of this system is almost zero. Pulse operation requires a strong voltage to generate a rising current. Once the current reaches the flat top, the load voltage will drop to a quite small value rapidly, and the current error of power supply must be kept within 10 ppm (parts per million) during this large dynamic range [13].

Superconducting coils will be adopted in part of the dipole magnets in HIAF, which require the magnetizing superconducting power supply working in pulse operation to satisfy the needs of HIAF. As the magnet power supply adopted superconducting coil works in the pulse mode, the rising or falling time of current is 2 seconds, and the flat top current can reach up to 8000 A. When the current pulse drops, the energy stored in the superconducting magnet needs to be transferred properly from the magnet to meet the requirement of the system. Normally, the energy of the magnet can be stored in an electrolytic capacitor or dissipated by an applied resistor. Nevertheless, for the series-

connected superconducting magnets of HIAF, the inductance of the magnet is very large. The huge energy cannot be disposed by conventional methods of electrolytic capacitor transfer or resistance depletion. Therefore, it is necessary to adopt new technologies to feed energy back to the grid. That is to say, the load of the system should be able to exchange energy with the grid and the stored excess energy should be returned to the grid in time. The magnet power supply is supposed to have the function of bidirectional energy flow [14, 15]. Meanwhile, to improve the beam quality of the new generation of HIAF further, many challenging requirements of magnet power supply of HIAF need to be studied in more depth. In addition to stability and ripple, more stringent requirements on the dynamic response speed are coming up with [10].

For the research of superconducting magnet power supply, a superconducting dipole magnet of the ion accelerator storage ring is studied and designed, and the magnetic field and electromagnetic force of the superconducting magnet are analyzed [13]. In the cited literature [16], a multiphase multiple magnet power supply based on the Buck chopper circuit is studied against the requirements of superconducting magnet power supply. However, based on the topology, the energy of the power supply cannot achieve bidirectional flow. Nor do the topology restrain disturbance of the magnet power supply effectively. The disturbance of the magnet power supply may lead to the quenching of the superconducting magnet, which will seriously affect the normal operation of the superconducting magnet and even destroy it. Therefore, the high precision and robustness of the superconducting power supply is also required [17]. Since energy feedback cannot be realized when the driving load of the superconducting magnet in the mentioned power supplies, an additional energy feedback unit is necessary. Meanwhile, the capacitor on DC side also causes dynamic response of the power supply system too slow to meet the requirements of dynamic performance of the superconducting magnet. Aimed at the above issues, the key point for the superconducting magnet system of the ion accelerator is to seek a magnet power supply scheme which can provide high-precision output current, bidirectional energy flowage, and excellent performance of grid side.

However, the current converter topology of magnet power supply cannot solve the above issues properly, so new technologies need to be introduced to improve it. The first is to solve the problem of low power factor on grid side, and then relevant research on energy feedback to the grid for superconducting power supply is urgently needed.

The matrix converter (MC) emerged in recent years provides a solution. The matrix converter can be applied to DC magnet power supply of ion accelerators when working in a rectification operation mode. Matrix converter with favorable dynamic performance, occupying small space, needs no energy storage component of large capacity on the DC side. With the matrix converter worked as a rectifier, sinusoidal input current can be realized so as to achieve high-power factor. Moreover, the matrix converter can also be utilized for the pulse magnet power supply of ion

accelerators. Bidirectional flowage of energy in the matrix converter can transmit excessive energy of the magnet back to the grid [18–20].

The study is a continuation of our preliminary researches [21, 22]. Since the performance of accelerator power supply largely depends on the choice of main circuit topology and control strategy [23, 24], the matrix converter and its novel modulation strategy proposed in the article based on practical current-type magnetizing power supply are a prospective solution to the above problems.

2. Three Implementation Alternatives

Taking the demand of power supply into account, a simpler three-phase input/one-phase output matrix converter (31 MC) is studied. Much attention is paid on the DC mode output of 31 MC without neutral line in this research. In this case, it is also called matrix rectifier (MR). According to the actual situation of the accelerator magnet power supply, three implementation alternatives are proposed.

The first is a direct-coupled MR. The MR is directly connected to the load, with input current and output current controlled by appropriate modulation strategies.

The second is a magnetic-coupled MR. Considering the problem of energy feedback in the falling segment of pulse in the superconducting magnet power supply, the MR is utilized as the prestage rectifier of the two-stage matrix converter (TSMC), while a virtual inverter is added as poststage to ensure bidirectional energy transmission. This approach is also equivalent to a reduced matrix converter.

The third is a preceding regulated MR. In view of possible existing deficiencies, the direct-coupled MR is only utilized as the prestage voltage regulator to control the input current waveform. The DC constant voltage outputted by MR will be applied to post-H-bridge to control the output current. The scheme will be studied further in this study.

The switching power supply based on H-bridge topology can be operated in a variety of working states by adopting a phase-shifting full-bridge control mode. Bipolar DC/pulse current waveform can be outputted when the H-bridge is working as a chopper, which is suitable for the operation of the accelerator system, such as quadrupole magnet and sextupole magnet. As shown in Figure 1, in the traditional topology of switching power supply, a diode rectifier bridge and a following second-order LC filter are generally utilized as a prestage of the H-bridge [6].

The prestage, whose output is equivalent to an ideal voltage source, can cause serious pollution to the grid. Aimed at the problem, a preceding regulated MR topology is proposed. Using a space vector modulation strategy, AC/DC conversion can be realized by the MR, with the input filter filtering out high frequency harmonics to ensure the “green” input performance. The DC side of the MR is connected to the classical H-bridge, whose output is joined with a filter and a magnet load. As post-stage, the H-bridge can realize accurate control of output current to obtain excellent output quality.

3. The Control Strategy of MC Applied to Accelerator Power Supply

3.1. Grid Side Space Vector Modulation Strategy. For the preceding regulated MR, an appropriate control strategy needs to be applied to both preceding stage and poststage. The matrix converter is preceding stage, in which space vector modulation (SVM) of input current is applied in order to obtain sinusoidal input current waveform and high input power factor [25, 26]. Here, the preceding stage can be virtual as a rectifier.

3.2. SVM without Zero Vector. Assuming that the input voltage is balanced, in order to obtain the maximum positive DC voltage at the DC side and ensure the input current is highly sinusoidal, the input phase voltage is divided into 6 sectors in each period [27]. In each sector, the voltage of one phase has the maximum absolute value and the polarity of the other two phases is opposite, as shown in Figure 2.

The space vectors of the rectifier stage are composed of six effective vectors and three zero vectors (I_{aa} , I_{bb} , I_{cc}), as shown in Figure 3. For example, in sector 1, the reference current vector I_{ref} is synthesized by I_{ab} and I_{ac} . To generate effective vectors I_{ab} and I_{ac} , the positive pole P on the DC side is always connected with phase a , and the negative pole N on the DC side is connected with phase b and c , respectively, which are utilized for modulation. In the first sector, the duty cycle of effective vector d_γ and d_δ of the rectifier stage can be deduced according to Figure 3, as shown in formula (1)

$$\begin{aligned} d_\gamma &= m_I \sin(60^\circ - \theta_{in}), \\ d_\delta &= m_I \sin \theta_{in}, \end{aligned} \quad (1)$$

where m_I is the modulation depth of rectifier stage adjustment system and θ_{in} is the angle between the reference current vector I_{ref} and its neighbor vector I_{ab} .

In order to obtain the maximum voltage utilization, zero vector will not be considered. Here, the switching state is synthesized of only two effective vectors I_{ab} and I_{ac} , namely, $d_{ab} + d_{ac} = 1$, so the duty cycle in a switching cycle is

$$\begin{aligned} d_{ab} &= \frac{d_\gamma}{d_\gamma + d_\delta}, \\ d_{ac} &= \frac{d_\delta}{d_\gamma + d_\delta}. \end{aligned} \quad (2)$$

The average output voltage of the DC side is

$$\begin{aligned} \bar{u}_{pn} &= d_{ab}u_{ab} + d_{ac}u_{ac} \\ &= \frac{3u_I}{2|\cos(\omega_I t)|}, \end{aligned} \quad (3)$$

where ω_I refers to the fundamental frequency of the input voltage.

Similarly, the switch states of all sectors of rectification stage in a pulse-width modulation (PWM) cycle can be obtained from the above analysis, as shown in Table 1.

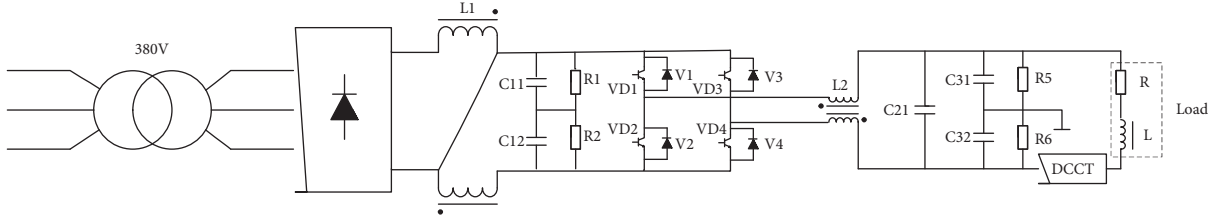


FIGURE 1: Topology of switching power supply based on H-bridge.

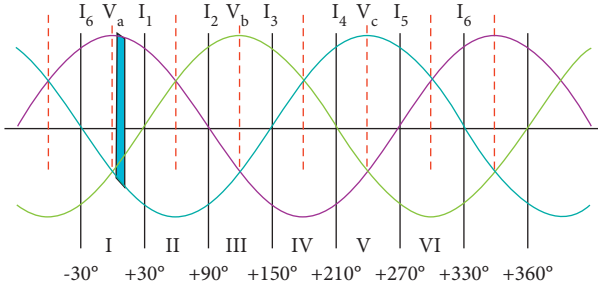


FIGURE 2: Division of input phase voltage sectors.

TABLE 1: Switch states of rectifier stage.

Sectors	Angle	Switch turned on	Modulation switch	DC side voltage
1	$-\pi/6 \sim \pi/6$	S_{ap}	S_{bn}, S_{cn}	u_{ab}, u_{ac}
2	$\pi/6 \sim \pi/2$	S_{cn}	S_{ap}, S_{bp}	u_{ac}, u_{bc}
3	$\pi/2 \sim 5\pi/6$	S_{bp}	S_{an}, S_{cn}	u_{ba}, u_{bc}
4	$5\pi/6 \sim 7\pi/6$	S_{an}	S_{bp}, S_{cp}	u_{ba}, u_{ca}
5	$7\pi/6 \sim 9\pi/6$	S_{cp}	S_{bn}, S_{an}	u_{cb}, u_{ca}
6	$3\pi/2 \sim 11\pi/6$	S_{bn}	S_{ap}, S_{cp}	u_{ab}, u_{cb}

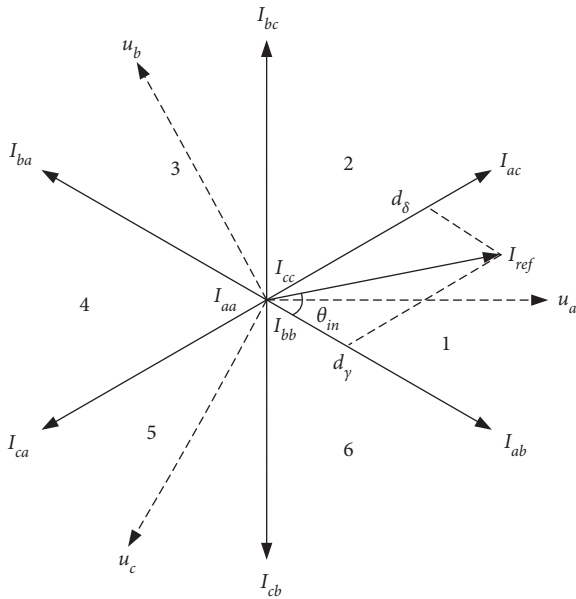


FIGURE 3: Space vector synthesis of rectification stage.

3.3. *SVM with Zero Vector*. The sector division and vector synthesis of the SVM with zero vector is similar to the SVM without zero vector, which will not be described again. For the SVM with zero vector, because of the addition of zero vector in vector synthesis, the voltage ratio will decrease, but the fluctuation of output is smaller than the SVM without zero vector.

3.4. *Control Strategy of Load Side in Accelerator Power Supply*. No matter accelerator power supply works in the DC mode or pulse mode, the control target of the power is load current. A series of indicators of the load current waveform are focused on, such as the stability of DC power supply and the tracking error of pulse power supply [28, 29]. It is very

important for power supply's normal operation and satisfactory performance obtained to choose suitable control method based on topology model of power supply.

In the topology scheme of the preceding regulated MR, constant DC output voltage of the preceding stage is provided to the magnet load after H-bridge and filtering. Considering the requirements of DC magnet power supply, meanwhile ensuring that load current keep track of the instruction current waveform, based on the analysis of control strategy of the matrix converter, the current SVM of the preceding stage and proportional integral (PI) feedback control of load current is combined as a feasible solution, and its schematic diagram is shown in Figure 4. Control variables can be obtained by PI calculation of difference value between load current and instruction current. In order to eliminate deviation and make the output follow the given value, a control variable is utilizable to adjust the rectifier modulation ratio of the preceding stage. Input current can be improved by using the current SVM, and output current can keep reliable track of instruction current by using PI regulation. The method is simple and with commendable robustness [30–32].

4. Modeling of Control Strategy with Different Topology

In Section 2, three kinds of applicable topology schemes are mentioned, and the third one is the preceding regulated MR. In order to test the alternative scheme, the closed-loop control simulation is carried out.

Simulation parameters are as follows:

- (1) Input voltage: three-phase nominal voltage: 380 V (+10%, -15%);
- (2) Parameters of the input filter: $R_f = 1.1 \Omega$, $L_f = 0.141 \text{ mH}$, $C_f = 60 \text{ uF}$;

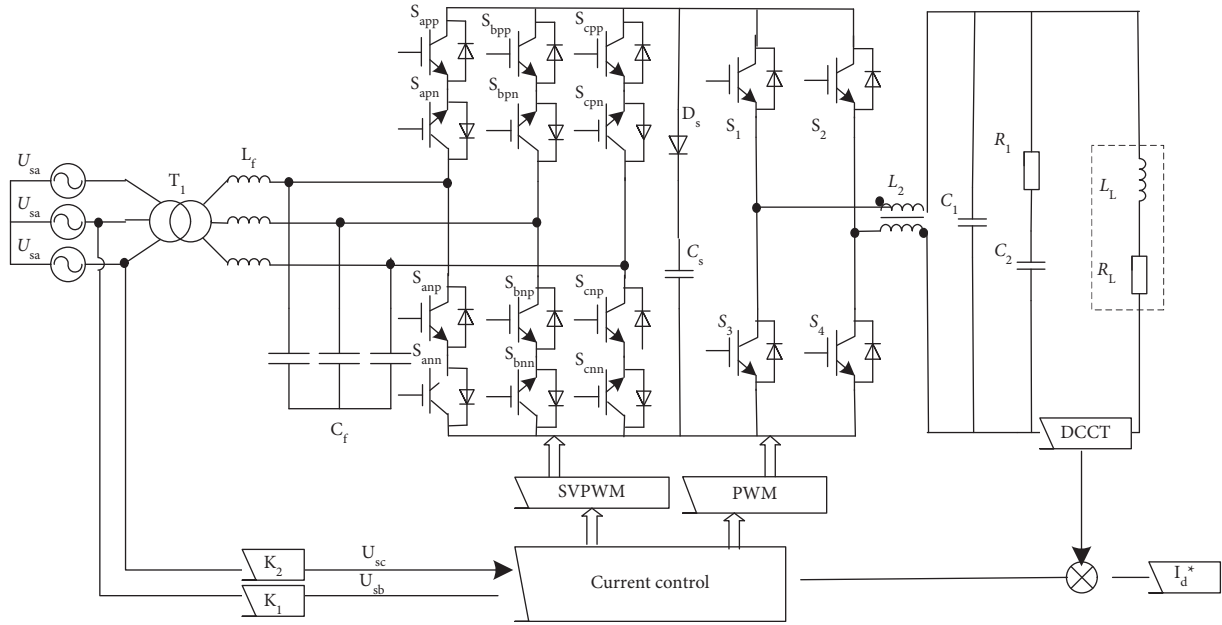


FIGURE 4: Preceding regulated matrix converter topology and control strategy.

- (3) Parameters of the output filter are: $L_1 = 7$ mH, $L_2 = 7$ mH, $C_1 = 450$ μ F, $R_1 = 1$ Ω , $C_2 = 100$ μ F;
- (4) Load parameters: $L_L = 1$ mH, $R_L = 0.5$ Ω ;
- (5) Simulation software: MATLAB 2018a;
- (6) Simulation mode: discrete simulation mode, simulation step size is $1e-6$ s.

In the preceding regulated MR topology, as the front stage of the H-bridge, the output of the matrix rectifier is constant DC voltage, with the magnet load connected to the output of the H-bridge. The simulation model is shown in Figure 5. The driving pulse generation of six power switches is shown in Figure 6.

Figure 7 shows the input voltage and current waveform. According to the waveform, it can be observed that the grid side power factor is higher, but the input current waveform is slightly worse, which may be due to unreasonable design of related full-bridge switches. From the amplitude-phase pattern as shown in Figure 8, it can be learned that the input current is ahead of the input voltage due to the presence of the input filter.

Figure 9 shows the output current waveform. According to the waveform, the output current reaches the set value of 200 A with little ripple.

When the conduction angle of H-bridge is 0, the input voltage and current waveform are shown as Figure 10. In Figure 10, the input current is more sinusoidal and the power factor is higher compared with the two variables in Figure 7.

From the amplitude-phase pattern as shown in Figure 11, it can be learned that without regulation of the feedback output current, the phase lead of input current relative to input voltage is less than the one in Figure 8.

Figure 12 shows the corresponding output current waveform. In the figure, when the conduction angle of

H-bridge is 0, the output current can be stabilized near 200 A by appropriate adjustment of parameters. However, the rise time becomes longer because it is not regulated by the feedback of the output current.

5. Experiment

5.1. Output Performance. A prototype of matrix rectifier DC magnet power supply is constructed with adopting the preceding regulated MR topology scheme. In the prototype, IGBT K30H603HAJ108 is selected to constitute bidirectional switches, DSP2812 is selected as the system control device, and CPLD EPM240T100C5N is selected to generate drive pulses and realize the commutation logic.

Experimental verification is carried out on a matrix power prototype based on the scheme of preceding regulated MR type. The structure is voltage regulator (maximum power 6 kVA), three-phase LC (1000 μ F, 2.5 mH), MR rectifier (preceding stage, current closed-loop control, voltage open loop control, 20 kHz), C filter (2200 μ F), H-bridge (poststage, 15 A/15 V, analog, adjustable duty cycle, 10 kHz), and load (1 ohm).

When the output current on the load is 6.2 A, as the preceding stage, MR maintains a constant output voltage of 23.6 V. At this time, the root mean square value (RMS) of the voltage-regulator output voltage (star connection) is 37.8 V, as shown in Figure 13 (the ratio of values shown in the figure is one in ten). The text description in Figure 13 is shown in Table 2.

5.2. Power Quality Analysis of Grid Side. For the preceding regulated MR in the scheme, the power factor tester PSL PQube is applied for a power factor test of the grid side.

When load current (Unit: Ampere) changes from small to large, the A-phase power factor, line voltage U_{AB} , total

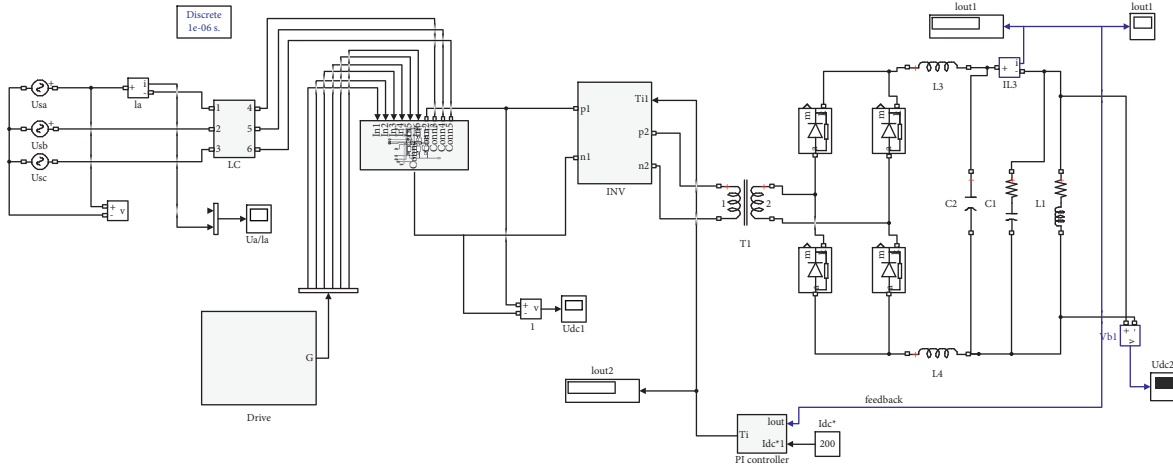


FIGURE 5: Simulation model of the preceding regulated MR.

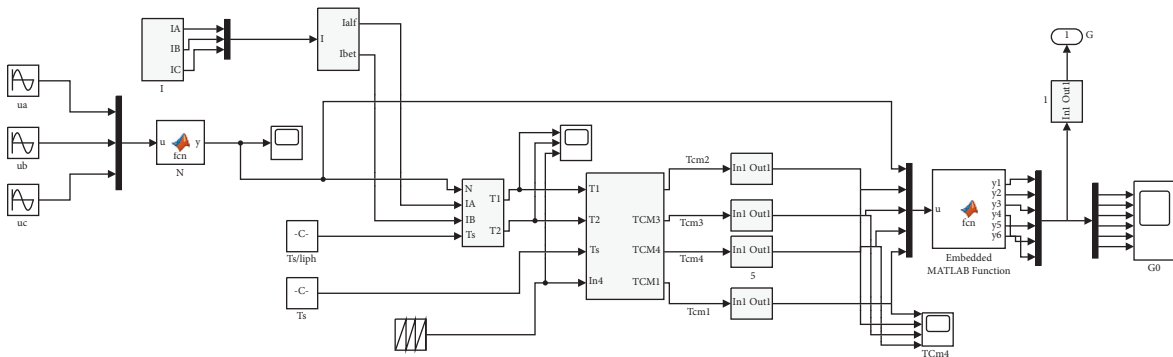


FIGURE 6: Driving pulses generation of the preceding regulated MR.

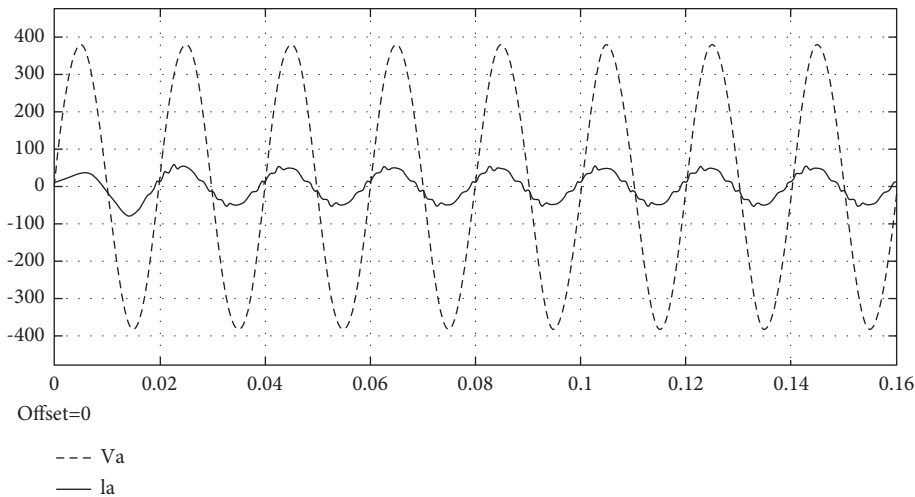


FIGURE 7: Input voltage and current waveform.

harmonic distortion rate (THD) of voltage, and total demand distortion rate (TDD) of current on the output side of the voltage regulator are shown in Figures 14~17, respectively. The corresponding current values (unit: ampere) of each section are 4, 5, 6, 7, 8, 8.5, 9, 9.5, 10, and 10.5.

It can be seen from Figure 14 that when the load current changes in the range of 4 A to 10.5 A, the A-phase power factor of the output side of the voltage regulator remains in a very small range of 0.944 to 0.982, indicating that a higher power factor of the grid side can be achieved in the scheme.

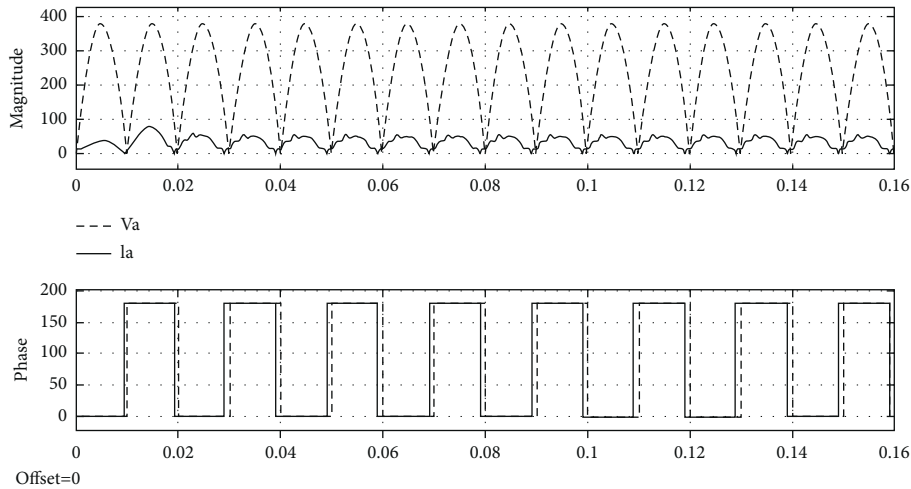


FIGURE 8: Input voltage and current waveform in amplitude-phase pattern.

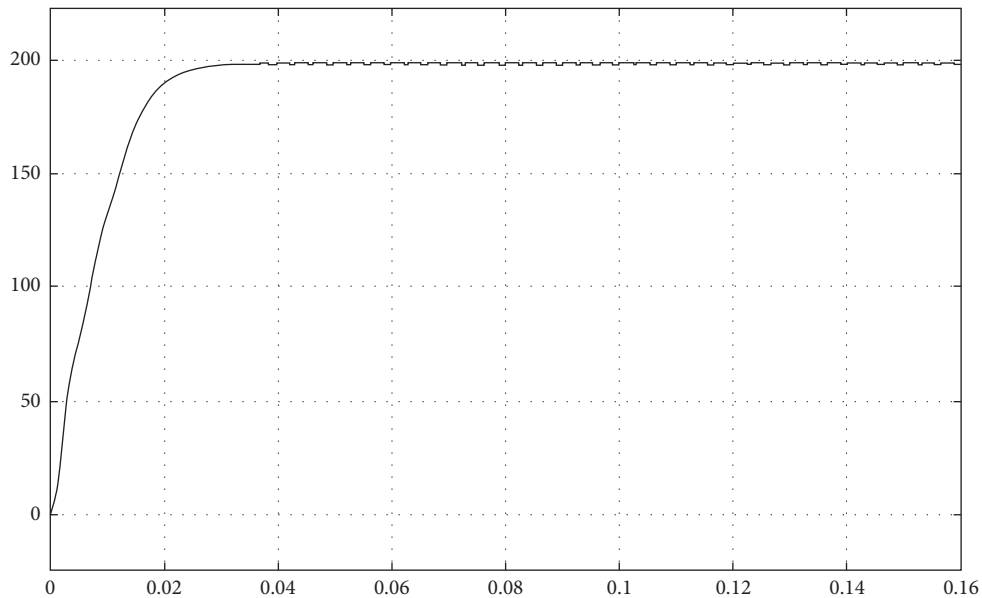


FIGURE 9: Output current waveform.

As shown in Figure 15, when the load current changes dramatically in a range of 4 A to 10.5 A, the output line voltage U_{AB} of voltage regulator only changes from 27.3 V to 24.5 V, with a relative change of only about 10%. It is demonstrated that load current varies over a wide range, which only needs the output of the grid side voltage regulator only adjusted slightly.

The THD is the RMS value of harmonic voltage divided by the RMS value of fundamental voltage. Under non-fault conditions, as the voltage will always be present, the correct reference will always be present. Hence, THD is an effective method to evaluate voltage distortion.

However, THD can be misleading when evaluating current distortion. It is because THD calculation of current

is based on fundamental current, which changes throughout the recording process as loads in the grid system. Thus, TDD is introduced. The TDD value is equal to the RMS value of harmonic current divided by the RMS value of rated current (or maximum demand current), similar to THD. It means that even if the fundamental current changes due to load, the TDD value does not give misleading results, but a better idea of how much harmonic distortion affects the system in depth.

It can be seen from Figures 16 and 17 that the THD of voltage does not exceed 0.3% and the TDD of current does not exceed 24% when the load current varies drastically from 4 A to 10.5 A.

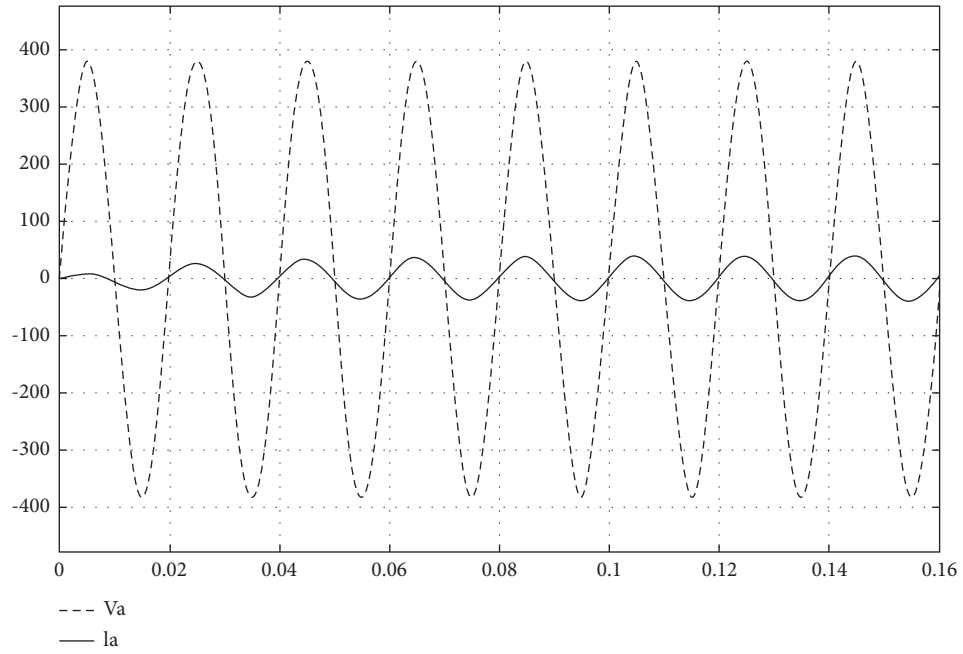


FIGURE 10: Input voltage and current waveform when the conduction angle of H-bridge is 0.

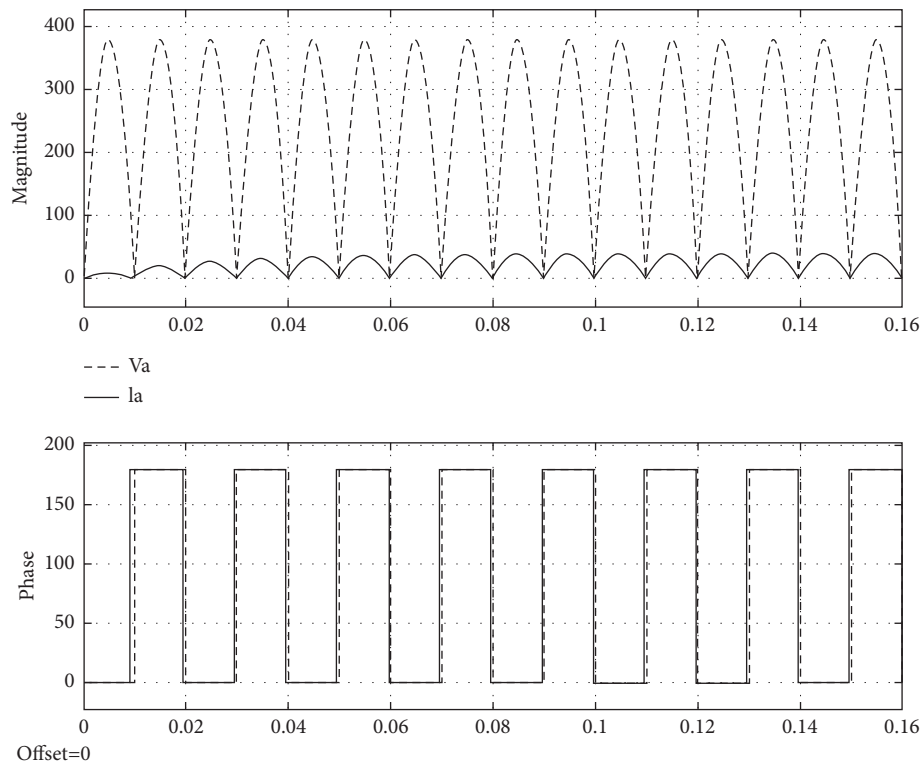


FIGURE 11: Input voltage and current waveform in amplitude-phase pattern when the conduction angle of H-bridge is 0.

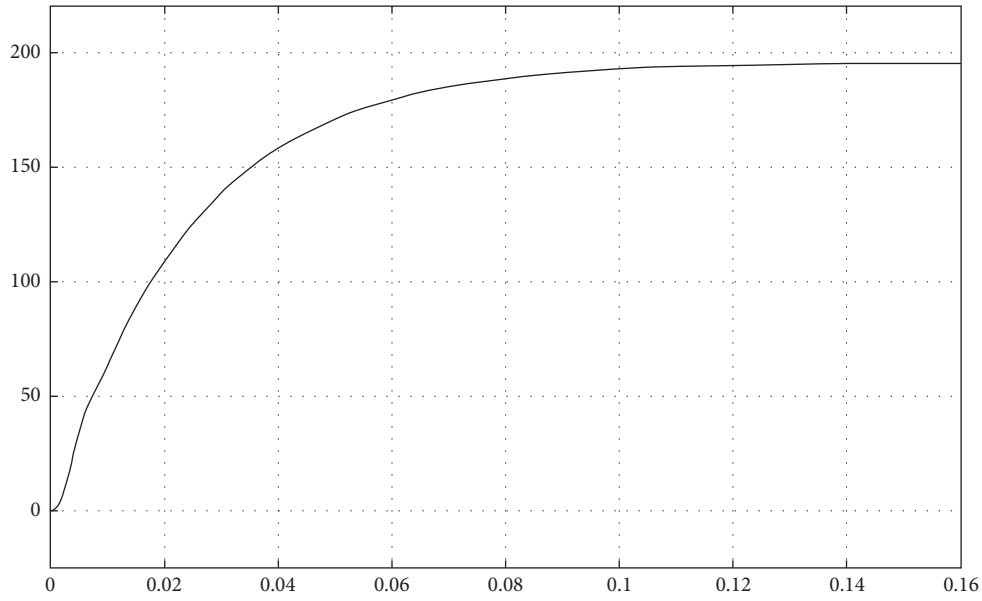


FIGURE 12: Output current waveform of when the conduction angle of H-bridge is 0.

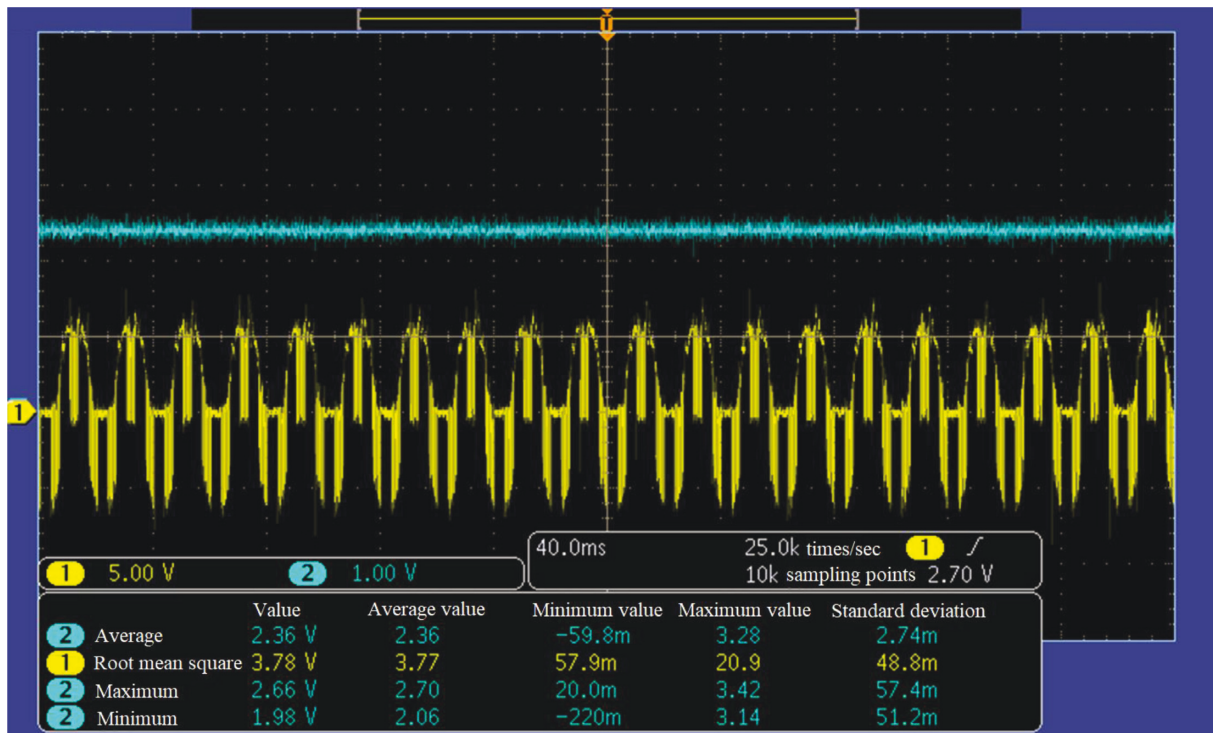


FIGURE 13: Preceding MR output voltage and voltage-regulator output voltage.

TABLE 2: Text description in Figure 13.

	① 5.00 V	② 1.00 V	40.0 ms	25.0k times per second	10k sampling points	① 2.70 V
	Value	Average value	Minimum value	Maximum value	Standard deviation	
② Average	2.36 V	2.36	-59.8 m	3.28		2.74 m
① Root mean square	3.78 V	3.77	57.9 m	20.9		48.8 m
② Maximum	2.66 V	2.70	20.0 m	3.42		57.4 m
② Minimum	1.98 V	2.06	-220 m	3.14		51.2 m

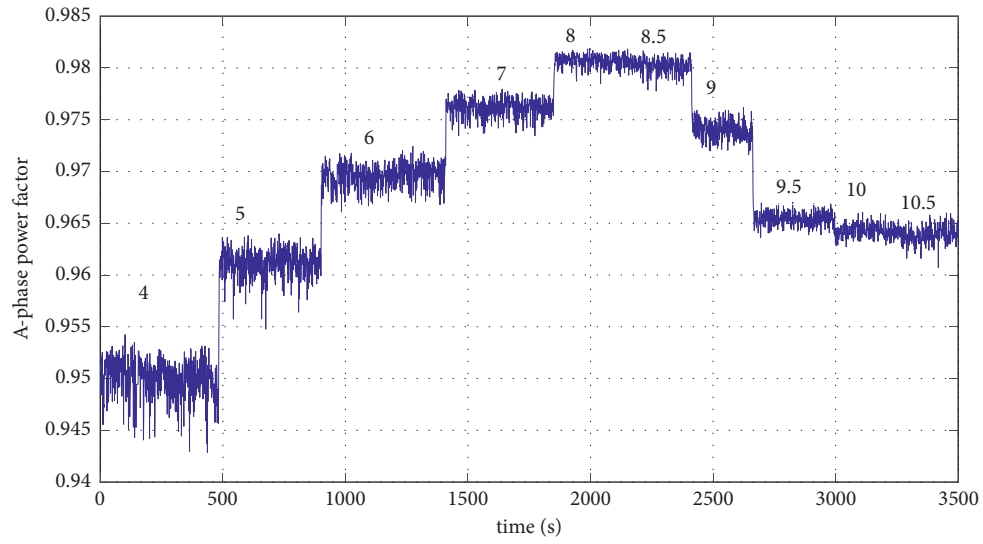


FIGURE 14: A-phase power factor.

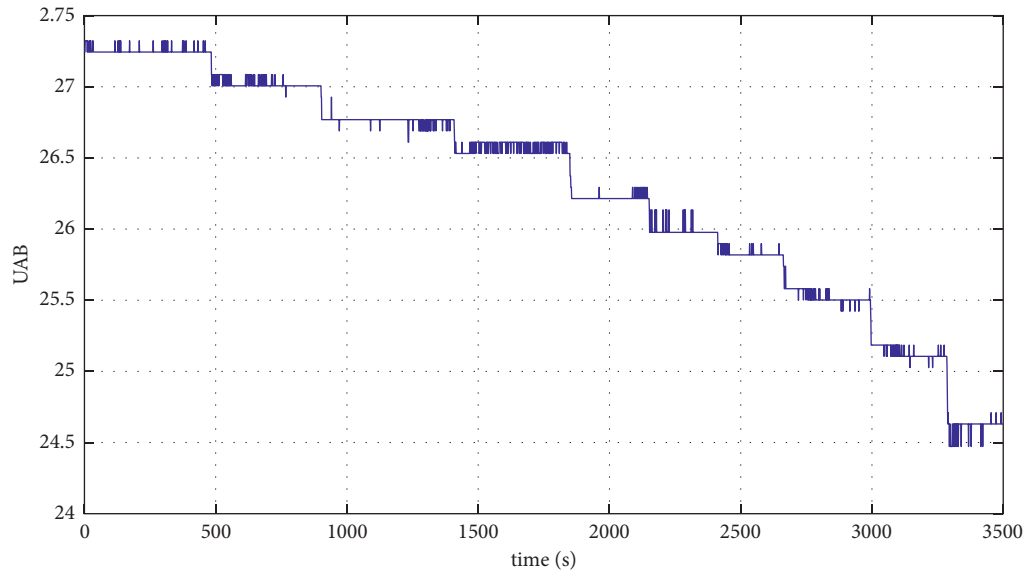
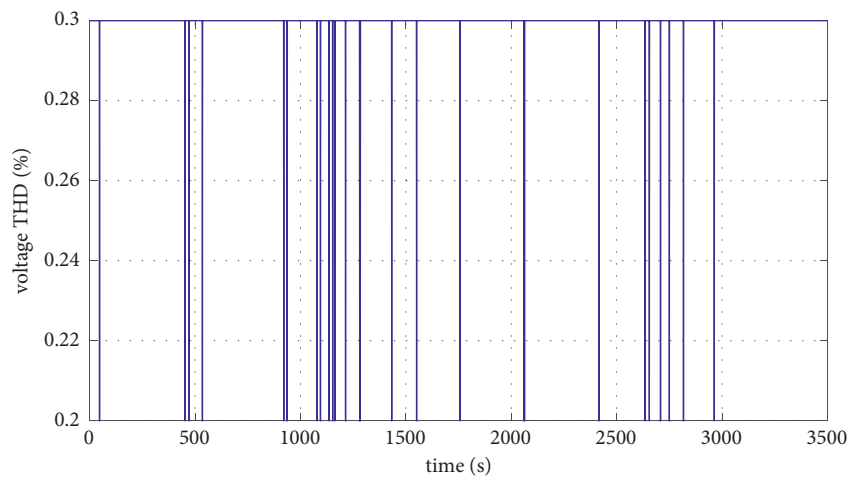
FIGURE 15: Line voltage U_{AB} .

FIGURE 16: Total harmonic distortion rate (THD) of voltage.

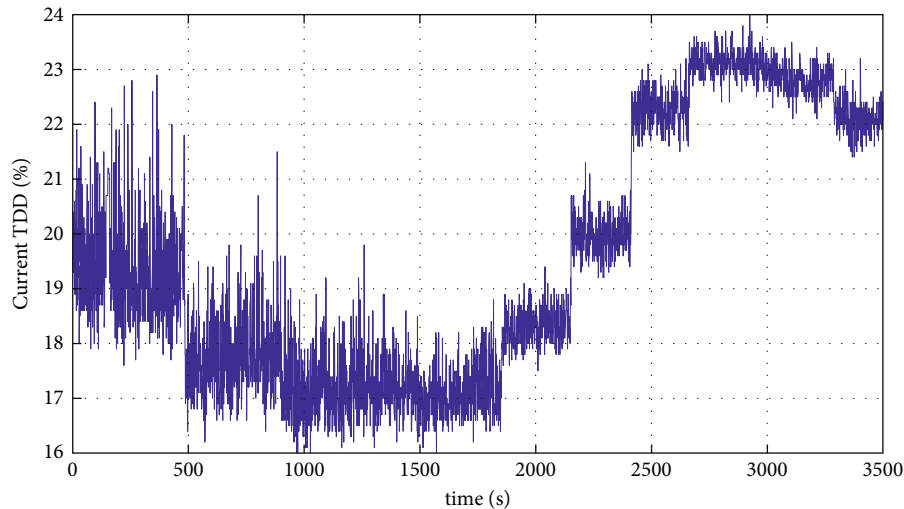


FIGURE 17: Total demand distortion rate (TDD) of current.

6. Conclusions

In this article, three types of matrix rectifier topology schemes suitable for accelerator magnet power supply are studied. According to the current status of accelerator steady current power supply and the excellent characteristics of a matrix converter, the preceding regulated MR is analyzed emphatically. The results of simulation and prototype experiments show that preceding regulated MR topology with proper modulation strategy can achieve steady current output and high-power factor on the grid side. The preceding regulated MR topology is validated basically suitable for DC power supply.

For conventional magnet power supplies of accelerator, H-bridge is quite mature. When it acts as a chopper, it can output DC or pulse current waveform. In the article, the matrix rectifier is substituted for its usual prestage and DC output mode is validated. In following research, the pulse output mode by adjusting the setting value will be carried out. However, the application of the topology to superconducting magnet power supply so as to feedback excessive energy still needs more research. Thus, it can be learned that the matrix converter has a promising application prospect in the field of accelerator special power supply.

Data Availability

No data were used to support this study.

Conflicts of Interest

The authors declare that there are no conflicts of interest regarding the publication of this paper.

Acknowledgments

This work is supported by National Natural Science Foundation (NNSF) of China (Grants 61867005, 11805156, and 51877176), Natural Science Foundation of Ningxia

Province (Grant 2020AAC03068), and Natural Science Foundation of Qinghai Province (Grant 2019-ZJ-948Q).

References

- [1] Q. Li and L. Sihver, "Therapeutic techniques applied in the heavy-ion therapy at IMP," *Nuclear Instruments and Methods in Physics Research Section B: Beam Interactions with Materials and Atoms*, vol. 269, no. 7, pp. 664–670, 2011.
- [2] X. Yang, H. Chen, J. Chen, Y. Qiao, and L. Ma, "Application status and development trends of medical proton and heavy ion accelerators," *Chinese Journal of Medical Instrumentation*, vol. 43, no. 1, pp. 37–42, 2019.
- [3] P. A. Seidl, "Inertial confinement fusion-experimental physics: heavy ion beam drive," *Encyclopedia of Nuclear Energy*, pp. 724–738, 2021.
- [4] H. Li, H. Ding, and Y. Yuan, "Design of a 60T dual-coil quasi-continuous magnetic field system with a hybrid power supply," *IEEE Transactions on Applied Superconductivity*, vol. 24, no. 3, pp. 1–5, 2014.
- [5] Y. Y. Wang, D. Q. Gao, J. H. Ding, and L. F. Shi, "Development of power supply for HIRFL-CSR dipole magnet," *Atomic Energy Science and Technology*, vol. 44, no. 4, pp. 499–503, 2010.
- [6] Y. Z. Huang, Y. X. Chen, Z. Z. Zhou, and H. Yan, "Research and design of digital power supply for HIRFL-CSR sexupole magnet," *Nuclear Physics Review*, vol. 28, no. 3, pp. 296–299, 2011, In Chinese.
- [7] D. Wang, Y. Ren, M. Zhang, and X. Gao, "Design and analysis of the 16T superconducting magnet for CFETR strand test facilities," *Fusion Engineering and Design*, vol. 162, no. 9, Article ID 112097, 2021.
- [8] T. Dai, C. Zhou, J. Qin, L. He, and J. Li, "The design of power supply for HF MRI superconducting magnet," *Nuclear Instruments and Methods in Physics Research Section A: Accelerators, Spectrometers, Detectors and Associated Equipment*, vol. 978, no. 2, Article ID 164344, 2020.
- [9] N. Xiao-fei, B. Feng, W. Xian-jin et al., "2 K cryogenic system development for superconducting cavity testing of CiADS," *Cryogenics*, vol. 115, no. 1, Article ID 103247, 2021.

- [10] B. X. Gou and E. Ralf, "Proposal for a spin physics research at HIAF-BRing," *Nuclear Physics Review*, vol. 34, no. 135, pp. 551–556, 2017.
- [11] L. J. Mao, J. C. Yang, J. W. Xia et al., "Electron cooling system in the booster synchrotron of the HIAF project," *Nuclear Instruments and Methods in Physics Research Section A: Accelerators, Spectrometers, Detectors and Associated Equipment*, vol. 786, pp. 91–96, 2015.
- [12] Q. Guo, R. L. Wang, Y. Zhu et al., "Study on high JC and low AC loss NbTi/Cu5Ni superconducting wire for HIAF magnets in WST," *IEEE Transactions on Applied Superconductivity*, vol. 30, no. 4, pp. 1–4, 2020.
- [13] X. Zhang, B. Wu, Y. Chen et al., "The fast-pulsed superconducting dipole prototype magnet of HIAF at IMP," *IEEE Transactions on Applied Superconductivity*, vol. 26, no. 4, pp. 1–4, 2016.
- [14] G. Zhang, S. Dai, N. Song et al., "The construction progress of a High-Tc superconducting power substation in China," *IEEE Transactions on Applied Superconductivity*, vol. 21, no. 3, pp. 2824–2827, 2011.
- [15] M. Baumann and J. W. Kolar, "Parallel connection of two three-phase three-switch buck-type unity-power-factor rectifier systems with DC-link current balancing," *IEEE Transactions on Industrial Electronics*, vol. 54, no. 6, pp. 3042–3053, 2007.
- [16] X. T. Zhang, Y. Y. Wang, and H. D. Dang, "Research on high precision accelerator superconducting magnet power supply," *Electric Drive*, vol. 40, no. 10, pp. 49–52+76, 2010.
- [17] X. L. Guo and J. Cheng, "Application of wavelet-based active power filter in accelerator magnet power supply," *Chinese Physics C*, vol. 38, no. 11, pp. 117007–117090, 2014.
- [18] G. Petrauskas and G. Svinkunas, "Innovative filter topology for power grid protection from switching ripple harmonics produced by matrix converter," *Iranian Journal of Science and Technology, Transactions of Electrical Engineering*, vol. 43, no. S1, pp. 495–505, 2019.
- [19] X. Yang, L. Liao, Q. Yang, B. Sun, and J. Xi, "Limited-energy output formation for multiagent systems with intermittent interactions," *Journal of the Franklin Institute*, vol. 358, no. 13, pp. 6462–6489, 2021.
- [20] J. Jin, J. Li, D. Qin, and N. Cai, "Output formation tracking for networked systems with limited energy and aperiodic silence," *Chinese Journal of Aeronautics*, vol. 35, no. 7, pp. 274–288, 2022.
- [21] B. Wang, D. Q. Gao, and C. Diao, "Study on matrix converter topology applied to accelerator power supply," *Atomic Energy Science and Technology*, vol. 50, no. 12, pp. 2283–2288, 2016.
- [22] J. Xi, L. Wang, J. Zheng, and X. Yang, "Energy-constraint formation for multiagent systems with switching interaction topologies," *IEEE Transactions on Circuits and Systems I: Regular Papers*, vol. 67, no. 7, pp. 2442–2454, 2020.
- [23] W. Han, D. Li, B. Qin, X. Liu, and G. Li, "Design and test of the power supply for a fast kicker magnet," *IEEE Transactions on Applied Superconductivity*, vol. 30, no. 4, pp. 1–4, 2020.
- [24] Z. Wang, P. Fu, L. Huang et al., "Preliminary design of high-power magnet converter for CRAFT," *Plasma Science and Technology*, vol. 22, no. 4, pp. 045604–46122, 2020.
- [25] S. Yammine and H. Thiesen, "Modelling and control of the HL-LHC nested magnet circuits at CERN," in *Proceedings of the 2019 20th Workshop On Control And Modeling For Power Electronics (COMPEL)*, pp. 1–6, Toronto, Canada, June 2019.
- [26] H. M. Basri, K. Lias, and S. Mekhilef, "Digital predictive current control fed by three-level indirect matrix converter under unbalanced power supply condition," in *Proceedings of the 2019 International UNIMAS STEM 12th Engineering Conference (En Con)*, pp. 34–39, Kuching, Malaysia, August 2019.
- [27] H. Tan, F. Fortunato, I. Suh et al., "ITER magnet power conversion building construction and AC/DC converter installation," *Fusion Engineering and Design*, vol. 146, pp. 1891–1894, 2019.
- [28] X. L. Guo, B. Chen, C. Han, and Y. Gao, "Development of dipole magnet power supply for BEPC-II energy upgrading project," *Radiation Detection Technology and Methods*, vol. 3, no. 2, pp. 14–36, 2019.
- [29] Z. X. Cheng, G. Z. Wang, and Z. Y. Yin, "Plug-in hybrid electric vehicle integrated conversion system and charging control strategy based on modular multilevel matrix converter," *Automation of Electric Power Systems*, vol. 43, no. 21, pp. 148–154, 2019.
- [30] J. Rzaša, "Modulation strategy for multi-phase matrix converter with common mode voltage elimination and adjustment of the input displacement angle," *Energies*, vol. 13, no. 3, p. 675, 2020.
- [31] H. Guo, H. J. Ge, X. Y. Xu, and Y. Quan, "Fault-tolerant control and input current optimization of three-phase to single-phase matrix converter," *Electric Power Automation Equipment*, vol. 39, no. 7, pp. 70–77, 2019.
- [32] A. M. Nori and T. K. Hassan, "Modeling and simulation of quasi-Z-source indirect matrix converter for permanent magnet synchronous motor drive," *International Journal of Power Electronics and Drive Systems*, vol. 10, no. 2, pp. 882–899, 2019.